

# Chapter 3

## Design of Switched High-Gain Observer for Nonlinear Systems

### 3.1 Introduction

Estimating the states from output measurements in dynamic systems is an essential task in control theory. This Chapter focuses on the design of switched high-gain observer, where observer's states can be estimated to the actual states in a chosen desired/predefined time independently of system parameters or initial conditions. Such development is important as in most of the existing works the expression for settling time bound involves certain parameters or constants and is not entirely independent, and hence it may sometimes be difficult to attain desired convergence time.

The observer design can be categorized into exponential convergence, asymptotic convergence, finite-time convergence, and fixed-time convergence. The finite-time observer is introduced [31], where the convergence time is finite but depends on the system's initial conditions and tuning parameters. To overcome this limitation, fixed-time observer is developed [32], where the convergence time is invariant with respect to the initial values of the system but depends explicitly on the system's parameters. Although fixed-time observers outperform finite-time observers in terms of the system's initial values, finding a direct relation between the convergence time and tuning parameters remains a challenge. To address this issue, predefined-time stability is developed, where the system's state converges to the equilibrium point within the desired settling time, and the convergence time is independent of the initial conditions and tuning parameters [37, 39]. This concept

has been utilized in various control problems and applications [17, 38].

The motivation behind this chapter is the need for complete state information and the desired settling/convergence time, which may not be feasible in practice due to unavailable or expensive sensors. Hence, an alternative technique is required that can estimate all other states using a known state. Furthermore, the convergence time can be selected according to the designer's preferences.

The main contributions of this chapter are as follows:

1. A switched high-gain observer is designed such that the observer's state converges to the actual state within the desired settling time.
2. The proposed method is invariant to the homogeneity property, which eliminates the need for careful selection of homogeneity powers and weights. As a result, the computational complexity of the proposed switched high-gain observer-based method is significantly reduced as compared to existing methods [31, 40–42].
3. In the proposed approach, the system's gain varies linearly (rather than quadratically) with the order of the system. Consequently, the proposed method requires less gain value to stabilize the system than the existing method [31].

A brief outline of this chapter is organized as follows. Section 3.2 contains preliminaries and problem formulation of the high-gain observer. Section 3.3 presents switched high-gain observer followed by respective proof. Section 3.4 includes the simulation results of the Van der Pol oscillator circuit and the Genesio-Tesi chaotic system. Finally, Section 3.5 summarizes the chapter.

## 3.2 Preliminaries and Problem Formulation

Consider the nonlinear dynamical system

$$\begin{aligned} \dot{x} &= f(x, u); & x(t_0) &= x_0 \\ y &= h(x) \end{aligned} \tag{3.1}$$

where  $x \in \mathbb{R}^n$  denotes the state vector,  $u \in \mathbb{R}^r$  represents the control input,  $y \in \mathbb{R}$  indicates the measured output and  $t_0 \in \mathbb{R}_{\geq 0}$  is the initial time.

Suppose that the system (3.1) can be represented as:

$$\begin{aligned} \dot{x} &= F(x) + \sum_{j=1}^r G_j(x)u_j; & x(t_0) &= x_0 \\ y &= h(x) \end{aligned} \quad (3.2)$$

where the functions  $F$ ,  $h$  and  $G_j (j = 1, \dots, r)$  are assumed to be sufficiently continuous differentiable in a domain  $\mathbb{D} \subset \mathbb{R}^n$ . The mappings  $F : \mathbb{D} \rightarrow \mathbb{R}^n$  and  $G_j : \mathbb{D} \rightarrow \mathbb{R}^n$  are vector fields on  $\mathbb{D}$  and  $h : \mathbb{D} \rightarrow \mathbb{R}$  is the scalar function on  $\mathbb{D}$ .

**Remark 3** *Note that  $\mathbb{D}$  is a compact set which can be chosen by the designer based on the concerned system.*

**Assumption 1** *We assume that the system (3.2) is detectable, i.e., the information of the output  $y(t)$  on any finite time interval  $[t_0, t_f]$ ,  $t_f > t_0$  completely determines the initial state  $x(t_0)$ .*

If the nonlinear system (3.2) is observable, then, by using change of variables, it can be represented as follows:

$$z = \Psi(x) = \text{col} (h(x), L_f h(x), \dots, L_f^{n-1} h(x)) \quad (3.3)$$

where the function  $\Psi : \mathbb{D} \rightarrow \mathbb{R}^n$  is a diffeomorphism and  $L_f h(x) = \frac{\partial h(x)}{\partial x} f$ .

Now, by using change of variables, the system (3.2) can be written as observable canonical form (2.4).

**Assumption 2** *Assume the functions  $g_{i,j}$  and  $\phi$  are Lipschitz with constant  $k$  and  $u$  be the bounded input such that  $\|u\| \leq u_0 \in \mathbb{R}_{\geq 0}$ .*

We require the following lemmas to prove the switched high-gain observer with the desired time convergence, which will be very useful for proofing our proposed method.

**Lemma 4** [8]: *The positive-definite symmetric matrix  $S(\alpha)$  can be written in the following way,*

$$S(\alpha)_{i,j} = S(1)_{i,j} \frac{1}{\alpha^{i+j-1}}, \quad S^{-1}(\alpha)_{i,j} = S^{-1}(1)_{i,j} \alpha^{i+j-1} \quad (3.4)$$

where  $1 \leq i, j \leq n$ .

**Lemma 5** [38]: *For every  $z \in \mathbb{R}$ , the following condition holds*

$$-z (1 - e^{-z}) \leq -|z| (1 - e^{-|z|}). \quad (3.5)$$

### 3.3 Design of Switched High-Gain Observer

In this section, we will design the high-gain observer by applying a switching technique for the nonlinear system (2.4). Next, the sufficient condition for the Lyapunov stability will prove for the system (3.6) and (3.11).

The switched high-gain observer is presented into two parts. The first part is given when time  $t \in [t_0, t_s)$ . And, the second part is stated when the time  $t \geq t_s$ . For the region  $t \in [t_0, t_s)$ , the high-gain observer is introduced in (3.6). And, for the region  $t \geq t_s$ , the high-gain observer is switched and is presented in (3.11).

**Part A:** For the region  $t \in [t_0, t_s)$  :

In view of (2.4), we design a high-gain observer and it can be represented as follows:

$$\begin{aligned}\dot{\hat{z}}_1 &= \hat{z}_2 + l_1 \left( \sigma \epsilon_1 + \gamma \frac{(1 - e^{-\epsilon_1})}{(t_s - t)} \right) + \sum_{j=1}^r g_{1,j}(\hat{z}_1) u_j \\ \dot{\hat{z}}_2 &= \hat{z}_3 + l_2 \left( \sigma \epsilon_1 + \gamma \frac{(1 - e^{-\epsilon_1})}{(t_s - t)} \right) + \sum_{j=1}^r g_{2,j}(\hat{z}_1, \hat{z}_2) u_j \\ &\vdots \\ \dot{\hat{z}}_n &= \phi(\hat{z}_1, \dots, \hat{z}_n) + l_n \left( \sigma \epsilon_1 + \gamma \frac{(1 - e^{-\epsilon_1})}{(t_s - t)} \right) + \sum_{j=1}^r g_{n,j}(\hat{z}_1, \dots, \hat{z}_n) u_j\end{aligned}\tag{3.6}$$

where  $\gamma \in \mathbb{R}_{>1}$ ,  $\sigma$  is the positive constant, and  $t_s$  is the desired convergence time and the designer can explicitly choose this settling time  $t_s$ .

The gain values  $l_1, l_2, \dots, l_n$  are given as:

$$[l_1, l_2, \dots, l_n]^T = S^{-1}(\alpha) C^T\tag{3.7}$$

where  $S(\alpha)$  is positive-definite symmetric  $n \times n$  matrix having unique solution which satisfies the matrix equation [31]:

$$A^T S(\alpha) + S(\alpha) A + \alpha S(\alpha) - C^T C = 0\tag{3.8}$$

$$S(\alpha) = S^T(\alpha), \quad \alpha > 0\tag{3.9}$$

with  $A_{n \times n}$  being the anti-shift operator  $A : \mathbb{R}^n \rightarrow \mathbb{R}^n$ ,  $(A)_{i,j} = \delta_{i,j-1}$ ,  $1 \leq i, j \leq n$  [8].

Note that the explicit solution of (3.8) is given as [7]:

$$S(\alpha)_{i,j} = \frac{(-1)^{i+j} C_{i+j-2}^{j-1}}{\alpha^{i+j-1}}; \quad 1 \leq i, j \leq n\tag{3.10}$$

$$\text{where } \mathbf{C}_{i+j-2}^{j-1} = \frac{(j-1)!}{(j-1-(i+j-2))!(i+j-2)!}.$$

From Eqn. 3.6, it is evident that the dynamics of the observer states become undefined or infinite when time  $t$  equals the settling time  $t_s$ . This phenomenon is known as a singularity.

**Part B:** For the region  $t \geq t_s$  :

In this region, the term  $\gamma(1-e^{-\epsilon_1})/(t_s-t)$  is not present. Since, the term  $\gamma(1-e^{-\epsilon_1})/(t_s-t)$  is introduced only for the region  $t \in [t_0, t_s)$  (see Lemma 1). Then, the high-gain observer is switched into the following form:

$$\begin{aligned} \dot{\hat{z}}_1 &= \hat{z}_2 + l_1 \sigma \epsilon_1 + \sum_{j=1}^r g_{1,j}(\hat{z}_1) u_j \\ \dot{\hat{z}}_2 &= \hat{z}_3 + l_2 \sigma \epsilon_1 + \sum_{j=1}^r g_{2,j}(\hat{z}_1, \hat{z}_2) u_j \\ &\vdots \\ \dot{\hat{z}}_n &= \phi(\hat{z}_1, \dots, \hat{z}_n) + l_n \sigma \epsilon_1 + \sum_{j=1}^r g_{n,j}(\hat{z}_1, \dots, \hat{z}_n) u_j. \end{aligned} \tag{3.11}$$

For the system (3.6) and (3.11), the block diagram of the switched high-gain observer is presented in Figure 3.1. Note that the part of the Figure 3.1 shown in blue dotted box will not be present when  $t \geq t_s$ . In this figure, we have constructed both the actual system's states, denoted as  $z$ , and the observer's states, represented as  $\hat{z}$ . Based on the knowledge of state  $z_1$ , we have estimated the unmeasured states.

For the region  $t \in [t_0, t_s)$  :

From (2.4) and (3.6), the dynamics of the observation errors are represented as:

$$\begin{aligned} \dot{\epsilon}_1 &= \epsilon_2 - l_1 \left( \sigma \epsilon_1 + \gamma \frac{(1-e^{-\epsilon_1})}{(t_s-t)} \right) + \sum_{j=1}^r (g_{1,j}(z_1) - g_{1,j}(\hat{z}_1)) u_j \\ \dot{\epsilon}_2 &= \epsilon_3 - l_2 \left( \sigma \epsilon_1 + \gamma \frac{(1-e^{-\epsilon_1})}{(t_s-t)} \right) + \sum_{j=1}^r (g_{2,j}(z_1, z_2) - g_{2,j}(\hat{z}_1, \hat{z}_2)) u_j \\ &\vdots \\ \dot{\epsilon}_n &= \phi(z_1, \dots, z_n) - \phi(\hat{z}_1, \dots, \hat{z}_n) - l_n \left( \sigma \epsilon_1 + \gamma \frac{(1-e^{-\epsilon_1})}{(t_s-t)} \right) \\ &\quad + \sum_{j=1}^r (g_{n,j}(z_1, \dots, z_n) - g_{n,j}(\hat{z}_1, \dots, \hat{z}_n)) u_j. \end{aligned} \tag{3.12}$$

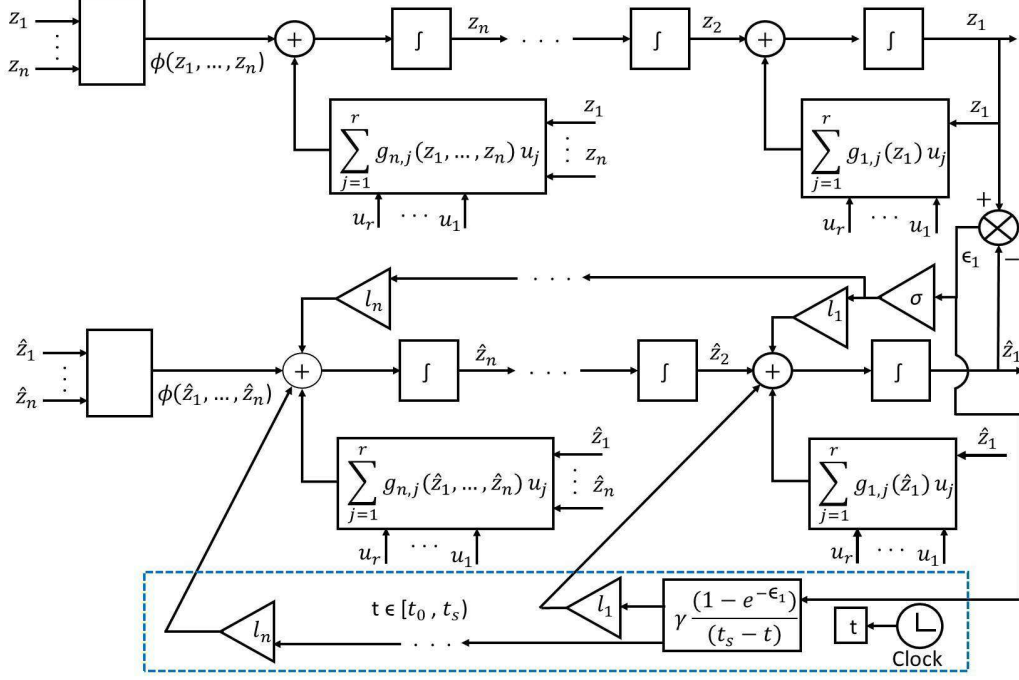


Figure 3.1: Block diagram of the switched high-gain observer.

Eq. (3.12) can also be represented as:

$$\begin{aligned}
 \begin{bmatrix} \dot{\epsilon}_1 \\ \dot{\epsilon}_2 \\ \vdots \\ \dot{\epsilon}_{n-1} \\ \dot{\epsilon}_n \end{bmatrix} &= \begin{bmatrix} \epsilon_2 \\ \epsilon_3 \\ \vdots \\ \epsilon_n \\ 0 \end{bmatrix} + \begin{bmatrix} 0 \\ 0 \\ \vdots \\ 0 \\ \phi(z_1, \dots, z_n) - \phi(\hat{z}_1, \dots, \hat{z}_n) \end{bmatrix} - \begin{bmatrix} l_1 \\ l_2 \\ \vdots \\ l_{n-1} \\ l_n \end{bmatrix} \left( \sigma \epsilon_1 + \gamma \frac{(1 - e^{-\epsilon_1})}{(t_s - t)} \right) \\
 &+ \begin{bmatrix} \sum_{j=1}^r (g_{1,j}(z_1) - g_{1,j}(\hat{z}_1)) u_j \\ \sum_{j=1}^r (g_{2,j}(z_1, z_2) - g_{2,j}(\hat{z}_1, \hat{z}_2)) u_j \\ \vdots \\ \sum_{j=1}^r (g_{n-1,j}(z_1, \dots, z_{n-1}) - g_{n-1,j}(\hat{z}_1, \dots, \hat{z}_{n-1})) u_j \\ \sum_{j=1}^r (g_{n,j}(z_1, \dots, z_n) - g_{n,j}(\hat{z}_1, \dots, \hat{z}_n)) u_j \end{bmatrix}. \quad (3.13)
 \end{aligned}$$

From (3.13), one can also rewrite the observation error dynamics into the following form:

$$\begin{aligned}
 \dot{\epsilon} &= A\epsilon - \sigma S^{-1}(\alpha) C^T \epsilon_1 - \gamma S^{-1}(\alpha) C^T \frac{(1 - e^{-\epsilon_1})}{(t_s - t)} + \varphi(z_1, \dots, z_n) - \varphi(\hat{z}_1, \dots, \hat{z}_n) \\
 &+ \sum_{j=1}^r (g_j(z_1, \dots, z_n) - g_j(\hat{z}_1, \dots, \hat{z}_n)) u_j \quad (3.14)
 \end{aligned}$$

where  $A = \begin{bmatrix} 0 & 1 & 0 & \cdots & 0 \\ 0 & 0 & 1 & \cdots & 0 \\ \vdots & \vdots & \vdots & \ddots & \vdots \\ 0 & 0 & 0 & 0 & 0 \end{bmatrix}_{n \times n}$ ,  $[l_1, l_2, \dots, l_n]^T = S^{-1}(\alpha)C^T$ ,  $\epsilon = [\epsilon_1, \epsilon_2, \dots, \epsilon_n]^T$ ,  
 $g_j(z_1, \dots, z_n) = [g_{1,j}(z_1), g_{2,j}(z_1, z_2), \dots, g_{n,j}(z_1, \dots, z_n)]^T$   
and  $\varphi(z_1, \dots, z_n) = [0, 0, \dots, \phi(z_1, \dots, z_n)]^T$ .

By substituting  $\epsilon_1 = C\epsilon$  in (3.14), one gets

$$\dot{\epsilon} = A\epsilon - \sigma S^{-1}(\alpha)C^T C\epsilon - \gamma S^{-1}(\alpha)C^T \frac{(1 - e^{-\epsilon_1})}{(t_s - t)} + (B(z, u) - B(\hat{z}, u)) \quad (3.15)$$

where  $(B(z, u) - B(\hat{z}, u)) = \varphi(z_1, \dots, z_n) - \varphi(\hat{z}_1, \dots, \hat{z}_n)$   
 $+ \sum_{j=1}^r (g_j(z_1, \dots, z_n) - g_j(\hat{z}_1, \dots, \hat{z}_n))u_j$ .

For the region  $t \geq t_s$  :

In this region, the term  $\gamma(1 - e^{-\epsilon_1})/(t_s - t)$  is not present. Then, in view of (2.4) and (3.11), the dynamics of the observation error  $\epsilon$  is written as:

$$\dot{\epsilon} = A\epsilon - \sigma S^{-1}(\alpha)C^T C\epsilon + (B(z, u) - B(\hat{z}, u)). \quad (3.16)$$

**Theorem 1** Consider the system (3.6) and (3.11). Suppose that the system (2.4) and input  $u$  holds the Assumptions 1 and 2. If there exist  $\gamma \in \mathbb{R}_{>1}$  and  $\alpha_1 \in (0, \infty)$ , such that the following inequality hold  $\gamma > \tau^2$  ( $\tau > 1$ ) and  $0 < \alpha < \alpha_1$ . Then, the observer's state converges to the actual state within the desired settling time.

*Proof:* The proof of the switched high-gain observer is presented into two parts.

**Part A:** For the region  $t \in [t_0, t_s)$ :

Let us consider the Lyapunov function as:

$$V(\epsilon) = \epsilon^T S(\alpha)\epsilon. \quad (3.17)$$

Taking time derivative of (3.17), one obtains

$$\dot{V}(\epsilon) = \epsilon^T S(\alpha)\dot{\epsilon} + \dot{\epsilon}^T S(\alpha)\epsilon. \quad (3.18)$$

In view of (3.15), we can write (3.18) as:

$$\begin{aligned} \dot{V}(\epsilon) = & \epsilon^T (A^T S(\alpha) + S(\alpha)A)\epsilon - 2\sigma \epsilon^T C^T C\epsilon - 2\gamma \epsilon^T C^T \frac{(1 - e^{-\epsilon_1})}{(t_s - t)} \\ & + 2\epsilon^T S(\alpha)(B(z, u) - B(\hat{z}, u)). \end{aligned} \quad (3.19)$$

Eq. (3.19) can also be written as:

$$\begin{aligned} \dot{V}(\epsilon) = & \epsilon^T (A^T S(\alpha) + S(\alpha)A - C^T C + C^T C) \epsilon - 2\sigma \epsilon^T C^T C \epsilon \\ & - 2\gamma \epsilon^T C^T \frac{(1 - e^{-\epsilon_1})}{(t_s - t)} + 2\epsilon^T S(\alpha) (B(z, u) - B(\hat{z}, u)). \end{aligned} \quad (3.20)$$

By substituting (3.8) in (3.20) and simplifying the equation, then one can represent (3.20) as:

$$\begin{aligned} \dot{V}(\epsilon) = & -\alpha \epsilon^T S(\alpha) \epsilon - (2\sigma - 1) \epsilon^T C^T C \epsilon - 2\gamma \epsilon^T C^T \frac{(1 - e^{-\epsilon_1})}{(t_s - t)} \\ & + 2\epsilon^T S(\alpha) (B(z, u) - B(\hat{z}, u)). \end{aligned} \quad (3.21)$$

Since  $\epsilon_1 = C\epsilon$  and in view of Lemma 1 and using  $\|z\|_{S(\alpha)}$  for  $(z^T S(\alpha) z)^{1/2}$ , one can write (3.21) as:

$$\begin{aligned} \dot{V}(\epsilon) \leq & -\alpha \|\epsilon\|_{S(\alpha)}^2 - (2\sigma - 1) \epsilon_1^2 - 2\gamma |\epsilon_1| \frac{(1 - e^{-|\epsilon_1|})}{(t_s - t)} \\ & + 2\|\epsilon\|_{S(\alpha)} \| (B(z, u) - B(\hat{z}, u)) \|_{S(\alpha)}. \end{aligned} \quad (3.22)$$

Eq. (3.22) can also be written as:

$$\begin{aligned} \dot{V}(\epsilon) \leq & -\alpha \|\epsilon\|_{S(\alpha)}^2 - (2\sigma - 1) \epsilon_1^2 - 2\gamma |\epsilon_1| \frac{(1 - e^{-|\epsilon_1|})}{(t_s - t)} \\ & + 2\|\epsilon\|_{S(\alpha)} ((B(z, u) - B(\hat{z}, u))^T S(\alpha) (B(z, u) - B(\hat{z}, u)))^{1/2}. \end{aligned} \quad (3.23)$$

By using quadratic form, i.e.,  $\zeta^T Q \zeta = \sum_{i,j} Q_{i,j} \zeta_i \zeta_j$  where  $Q$  is symmetric matrix, one obtains (3.23) as:

$$\begin{aligned} \dot{V}(\epsilon) \leq & -\alpha \|\epsilon\|_{S(\alpha)}^2 - (2\sigma - 1) \epsilon_1^2 - 2\gamma |\epsilon_1| \frac{(1 - e^{-|\epsilon_1|})}{(t_s - t)} \\ & + 2\|\epsilon\|_{S(\alpha)} \left( \sum_{i,j} S(\alpha)_{i,j} (B_i(\underline{z}_i, u) - B_i(\hat{\underline{z}}_i, u)) (B_j(\underline{z}_j, u) - B_j(\hat{\underline{z}}_j, u)) \right)^{1/2} \end{aligned} \quad (3.24)$$

where  $\underline{z}_i = [z_1, \dots, z_i]^T$  and  $B_i(\underline{z}_i, u) : \mathbb{R}^i \rightarrow \mathbb{R}$  (see [8] for the details of the last term of (3.24)).

Since  $g_{i,j}$  ( $i = 1, \dots, n, j = 1, \dots, r$ ) and  $\phi$  are Lipschitz with constant  $k$  and  $\|u\|$  is bounded by  $u_0$  (recall the previous Assumption 2). From (3.24),  $B_i(\underline{z}, u) : \mathbb{R}^i \rightarrow \mathbb{R}$  is Lipschitz with constant  $k_i$ .

Now, by using Lipschitz condition and Lemma 4, one can represented (3.24) as:

$$\begin{aligned} \dot{V}(\epsilon) \leq & -\alpha \|\epsilon\|_{S(\alpha)}^2 - (2\sigma - 1) \epsilon_1^2 - 2\gamma |\epsilon_1| \frac{(1 - e^{-|\epsilon_1|})}{(t_s - t)} \\ & + 2\|\epsilon\|_{S(\alpha)} \left( (u_0 + 1)^2 r^2 \sum_{i,j} \frac{S(1)_{i,j}}{\alpha^{i+j-1}} k_i \|\underline{\epsilon}_i\|_{\mathbb{R}^i} k_j \|\underline{\epsilon}_j\|_{\mathbb{R}^j} \right)^{1/2}. \end{aligned} \quad (3.25)$$

By setting  $k = \sup_i k_i$  and  $S = \sup_{i,j} |S(1)_{i,j}|$ , we obtain

$$\begin{aligned} \dot{V}(\epsilon) &\leq -\alpha \|\epsilon\|_{S(\alpha)}^2 - (2\sigma - 1)\epsilon_1^2 - 2\gamma|\epsilon_1| \frac{(1 - e^{-|\epsilon_1|})}{(t_s - t)} \\ &\quad + 2\|\epsilon\|_{S(\alpha)} \left( (u_0 + 1)^2 r^2 k^2 S \alpha \sum_{i,j} \left\| \frac{\epsilon_i}{\alpha^i} \right\|_{\mathbb{R}^i} \left\| \frac{\epsilon_j}{\alpha^j} \right\|_{\mathbb{R}^j} \right)^{1/2}. \end{aligned} \quad (3.26)$$

Let us assume  $\xi_i = \epsilon_i/\alpha^i$ . Clearly, one can write  $\left\| \frac{\epsilon_i}{\alpha^i} \right\|_{\mathbb{R}^i} \leq \|\xi_i\|_{\mathbb{R}^i} \leq \|\xi\|_{\mathbb{R}^n}$  (for  $\alpha \geq 1$ ). Eq. (3.26) can be rewritten as:

$$\begin{aligned} \dot{V}(\epsilon) &\leq -\alpha \|\epsilon\|_{S(\alpha)}^2 - (2\sigma - 1)\epsilon_1^2 - 2\gamma|\epsilon_1| \frac{(1 - e^{-|\epsilon_1|})}{(t_s - t)} \\ &\quad + 2\|\epsilon\|_{S(\alpha)} \left( k^2 n^2 (u_0 + 1)^2 r^2 S \alpha \|\xi\|^2 \right)^{1/2}. \end{aligned} \quad (3.27)$$

By using norm equivalence, if there exists  $\mu > 0$  such that  $\|\xi\|_{1,n}^2 \leq \mu \|\xi\|_{S(1)}^2, \forall \xi \in \mathbb{R}^n$ , then, by using  $\|\xi\|_{S(1)}^2 = \frac{\|\epsilon\|_{S(\alpha)}^2}{\alpha}$ , one can write (3.27) as:

$$\dot{V}(\epsilon) \leq -\alpha \|\epsilon\|_{S(\alpha)}^2 - (2\sigma - 1)\epsilon_1^2 - 2\gamma|\epsilon_1| \frac{(1 - e^{-|\epsilon_1|})}{(t_s - t)} + 2\mu kn(u_0 + 1)r\sqrt{S} \|\epsilon\|_{S(\alpha)}^2. \quad (3.28)$$

If there exists  $\tau > 1$ , such that the following inequality holds

$$\|\epsilon\|_{S(\alpha)} \leq \tau |\epsilon_1| \quad (3.29)$$

then, (3.28) can be expressed as:

$$\begin{aligned} \dot{V}(\epsilon) &\leq -\alpha \|\epsilon\|_{S(\alpha)}^2 - (2\sigma - 1) \frac{\|\epsilon\|_{S(\alpha)}^2}{\tau^2} - 2\gamma \frac{\|\epsilon\|_{S(\alpha)}}{\tau} \frac{\left(1 - e^{-\frac{\|\epsilon\|_{S(\alpha)}}{\tau}}\right)}{(t_s - t)} \\ &\quad + 2\mu kn(u_0 + 1)r\sqrt{S} \|\epsilon\|_{S(\alpha)}^2. \end{aligned} \quad (3.30)$$

In accordance with (3.17), we can rewrite (3.17) as:

$$V = \|\epsilon\|_{S(\alpha)}^2. \quad (3.31)$$

In view of (3.31), one can represent (3.30) as:

$$\begin{aligned} \dot{V} &\leq -\alpha V - (2\sigma - 1) \frac{V}{\tau^2} - 2\gamma \frac{\sqrt{V}}{\tau} \frac{\left(1 - e^{-\frac{\sqrt{V}}{\tau}}\right)}{(t_s - t)} + KV \\ &= -\left(\frac{2\sigma - 1}{\tau^2} - K\right) V - 2\gamma \frac{\sqrt{V}}{\tau} \frac{\left(1 - e^{-\frac{\sqrt{V}}{\tau}}\right)}{(t_s - t)}. \end{aligned} \quad (3.32)$$

where  $K = 2\mu kn(u_0 + 1)r\sqrt{S}$ .

Substituting  $\sigma > (K\tau^2 + 1)/2$  into (3.32) yields

$$\dot{V} \leq -2\gamma \frac{\sqrt{V}}{\tau} \frac{\left(1 - e^{-\frac{\sqrt{V}}{\tau}}\right)}{(t_s - t)}. \quad (3.33)$$

Let  $\varrho = \sqrt{V}/\tau$ , then the time derivative is

$$\dot{\varrho} = \frac{1}{\tau} \frac{1}{2\sqrt{V}} \dot{V} \leq -\frac{\gamma}{\tau^2} \frac{(1 - e^{-\varrho})}{(t_s - t)}.$$

It can also be written as:

$$\dot{\varrho} \leq -\gamma_0 \frac{(1 - e^{-\varrho})}{(t_s - t)}, \quad t_0 \leq t < t_s \quad (3.34)$$

where  $\gamma_0 = \gamma/\tau^2 > 1 \Rightarrow \gamma > \tau^2$ .

**Part B:** For the region  $t \geq t_s$ :

Consider the previous assumption

$$V(\epsilon) = \epsilon^T S(\alpha) \epsilon. \quad (3.35)$$

By taking time derivative of (3.35) along the solution of (3.16), one gets

$$\dot{V}(\epsilon) = -\alpha \epsilon^T S(\alpha) \epsilon - (2\sigma - 1) \epsilon^T C^T C \epsilon + 2\epsilon^T S(\alpha) (B(z, u) - B(\hat{z}, u)).$$

By using  $\|z\|_{S(\alpha)}$  for  $(z^T S(\alpha) z)^{1/2}$  and the results of [8], it can be written as

$$\begin{aligned} \dot{V}(\epsilon) &\leq -\alpha \|\epsilon\|_{S(\alpha)}^2 - (2\sigma - 1) \epsilon_1^2 + 2\|\epsilon\|_{S(\alpha)} \| (B(z, u) - B(\hat{z}, u)) \|_{S(\alpha)} \\ &= -\alpha \|\epsilon\|_{S(\alpha)}^2 - (2\sigma - 1) \epsilon_1^2 + 2\|\epsilon\|_{S(\alpha)} \left( \sum_{i,j} S(\alpha)_{i,j} (B_i(\underline{z}_i, u) - B_i(\hat{\underline{z}}_i, u)) \right. \\ &\quad \left. (B_j(\underline{z}_j, u) - B_j(\hat{\underline{z}}_j, u)) \right)^{1/2}. \end{aligned} \quad (3.36)$$

Since, for  $t \geq t_s$ , the term  $\gamma(1 - e^{-\epsilon_1})/(t_s - t)$  is not present. Then, the Eq. (3.32) becomes

$$\dot{V} \leq -\left(\frac{2\sigma - 1}{\tau^2} - K\right) V. \quad (3.37)$$

From the previous assumption, i.e.,  $\left(\frac{2\sigma - 1}{\tau^2} - K\right) > 0$ , then, we can write (3.37) as:

$$\dot{V} \leq -\lambda V; \quad \lambda = \left(\frac{2\sigma - 1}{\tau^2} - K\right). \quad (3.38)$$

According to the discussions, as mentioned above and invoking the Lemma 4, it is ensured that the (3.34) shows the desired time convergence where state  $\varrho$  converges to

zero within the desired settling time  $t_s$ . Thus, using (3.34), one obtains  $\varrho = 0$  for all  $t \geq t_s$ . Since  $\varrho = \sqrt{V}/\tau = 0$ , then one gets  $\epsilon = 0 \forall t \geq t_s$ . Hence, the observer's state converges to the actual state within the desired settling time  $t_s$ . The proof of Theorem 1 is completed. ■

**Remark 4** *In the proof of Theorem 1, we utilized the switching structure and predefined techniques. The switching structure plays a pivotal role in avoiding the singularity of the observer's state and achieving the desired convergence.*

### 3.4 Simulation Results

To verify the efficacy of the proposed approach, we have considered two practical nonlinear systems. The first system is the Van der Pol oscillator circuit, shown in Figure 3.2 (see [14]). The second system is the Genesio-Tesi chaotic system, illustrated in Figure 3.5 (see [34]).

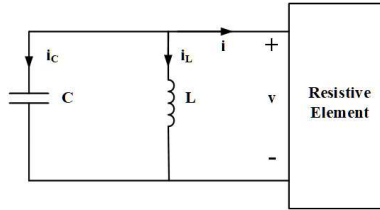


Figure 3.2: Van der Pol oscillator circuit.

**Example 1:** Let us consider the Van der Pol oscillator circuit [14]:

$$\begin{aligned} \dot{z}_1 &= z_2 \\ \dot{z}_2 &= -z_1 + 2(1 - z_1^2)z_2 \\ y &= z_1. \end{aligned} \tag{3.39}$$

The matrices  $S(\alpha)$  can be represented as follows [8]:

$$S(\alpha) = \begin{bmatrix} \frac{1}{\alpha} & -\frac{1}{\alpha^2} \\ -\frac{1}{\alpha^2} & \frac{2}{\alpha^3} \end{bmatrix}, \quad S^{-1}(\alpha) = \begin{bmatrix} 2\alpha & \alpha^2 \\ \alpha^2 & \alpha^3 \end{bmatrix}.$$

For the region  $t \in [t_0 \ t_s)$  :

In view of (3.6), the proposed switched high-gain observer for the Van der Pol oscillator

system (3.39) is given as:

$$\begin{aligned}\dot{\hat{z}}_1 &= \hat{z}_2 + l_1 \left( \sigma \epsilon_1 + \gamma \frac{(1 - e^{-\epsilon_1})}{(t_s - t)} \right) \\ \dot{\hat{z}}_2 &= -\hat{z}_1 + 2(1 - \hat{z}_1^2)\hat{z}_2 + l_2 \left( \sigma \epsilon_1 + \gamma \frac{(1 - e^{-\epsilon_1})}{(t_s - t)} \right)\end{aligned}$$

where  $l_1 = 2\alpha, l_2 = \alpha^2$  and  $\sigma$  are the tuning parameters.

For the region  $t \geq t_s$ :

In accordance with (3.11), the proposed observer is represented as:

$$\begin{aligned}\dot{\hat{z}}_1 &= \hat{z}_2 + l_1 \sigma \epsilon_1 \\ \dot{\hat{z}}_2 &= -\hat{z}_1 + 2(1 - \hat{z}_1^2)\hat{z}_2 + l_2 \sigma \epsilon_1.\end{aligned}$$

In the simulation, the initial conditions  $z(0) = [1.5 \quad -1]$  and the settling time  $t_s = 1$  sec. are assumed for Figures. 3.3 and 3.4. The gain values are considered as  $\alpha = 0.5$  and  $\gamma = 15$ , the initial observer's states  $\hat{z}(0) = [0.5 \quad 2]$  for Figure 3.3. For the simulation (in Figure 3.3),  $\sigma = 1.5$  is selected for  $t < t_s$  and  $\sigma = 10$  is taken for  $t \geq t_s$ . Similarly, for Figure 3.4, the gains  $\alpha = 1.5, \gamma = 12$  and the initial observer's states  $\hat{z}(0) = [2 \quad -5]$  are assumed. For  $t < t_s$ ,  $\sigma$  is selected as 1.5. For  $t \geq t_s$ ,  $\sigma$  is taken as 10. The simulation results is depicted in Figure 3.4. The time evolution of the observations error is shown in Figures. 3.3 and 3.4. It can be noticed that the initial observations error for both systems are different, and the convergence time is obtained within the same desired settling time ( $t_s = 1$  sec.).

**Example 2:** Let us consider the Genesio-Tesi chaotic system [34]:

$$\begin{aligned}\dot{z}_1 &= z_2 \\ \dot{z}_2 &= z_3 \\ \dot{z}_3 &= -az_1 - bz_2 - cz_3 + dz_1^2 \\ y &= z_1\end{aligned}\tag{3.40}$$

where  $a, b, c$  and  $d$  are the constant parameters such that  $ab > c$ . For the simulations, the constant parameters are assumed as  $a = R/R_3 = 1, b = R/R_4 = 1.1, c = R/R_5 = 0.44$  and  $d = R/(10R_6) = 1$ , where  $R$  is the change of variable parameter (see [34] for the details of the Eq. (3.40)).

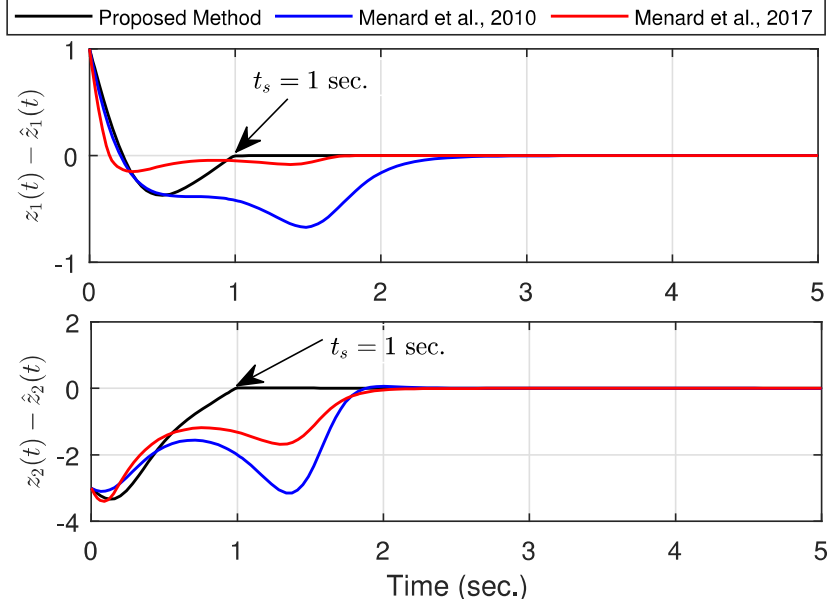


Figure 3.3: Observations error with  $t_s = 1$  sec., the initial observation states  $\hat{z}(0) = \begin{bmatrix} 0.5 & 2 \end{bmatrix}$ .

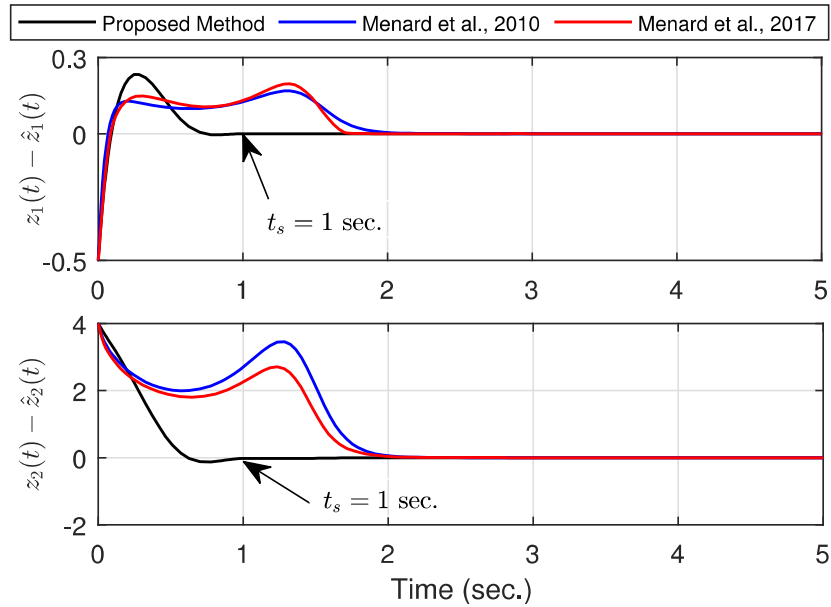


Figure 3.4: Observations error with  $t_s = 1$  sec., the initial observation states  $\hat{z}(0) = \begin{bmatrix} 2 & -5 \end{bmatrix}$ .

The matrices  $S(\alpha)$  can be represented as follows [42]:

$$S(\alpha) = \begin{bmatrix} \frac{1}{\alpha} & -\frac{1}{\alpha^2} & \frac{1}{\alpha^3} \\ -\frac{1}{\alpha^2} & \frac{2}{\alpha^3} & \frac{3}{\alpha^4} \\ \frac{1}{\alpha^3} & -\frac{3}{\alpha^4} & \frac{6}{\alpha^5} \end{bmatrix}, \quad S^{-1}(\alpha) = \begin{bmatrix} 3\alpha & 3\alpha^2 & \alpha^3 \\ 3\alpha^2 & 5\alpha^3 & 2\alpha^4 \\ \alpha^3 & 2\alpha^4 & \alpha^5 \end{bmatrix}.$$

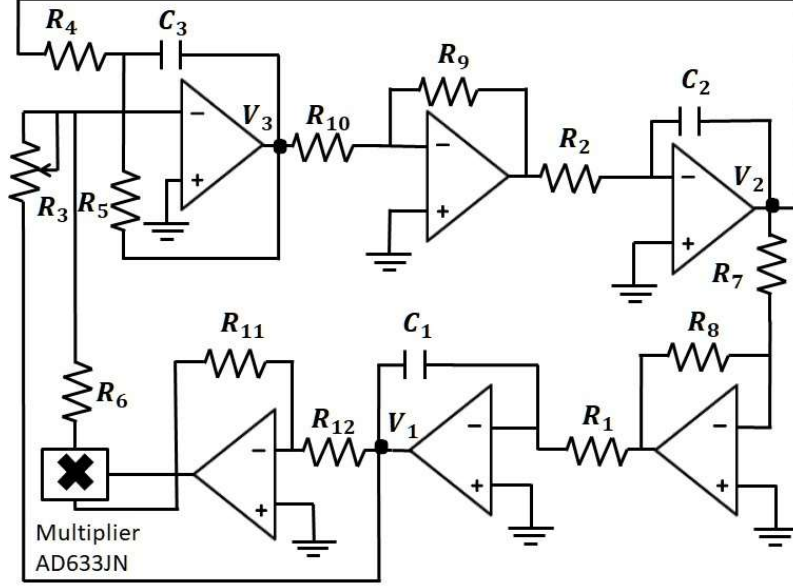


Figure 3.5: Circuit of Genesisio-Tesi.

For the region  $t \in [t_0 \ t_s)$  :

In view of (3.6), the proposed switched high-gain observer for the chaotic system (3.40) is given as:

$$\begin{aligned}\dot{\hat{z}}_1 &= \hat{z}_2 + l_1 \left( \sigma \epsilon_1 + \gamma \frac{(1 - e^{-\epsilon_1})}{(t_s - t)} \right) \\ \dot{\hat{z}}_2 &= \hat{z}_3 + l_2 \left( \sigma \epsilon_1 + \gamma \frac{(1 - e^{-\epsilon_1})}{(t_s - t)} \right) \\ \dot{\hat{z}}_3 &= -a\hat{z}_1 - b\hat{z}_2 - c\hat{z}_3 + d\hat{z}_1^2 + l_3 \left( \sigma \epsilon_1 + \gamma \frac{(1 - e^{-\epsilon_1})}{(t_s - t)} \right)\end{aligned}$$

where  $l_1 = 3\alpha$ ,  $l_2 = 3\alpha^2$ ,  $l_3 = \alpha^3$  and  $\sigma$  are the tuning parameters.

For the region  $t \geq t_s$  :

In accordance with (3.11), the observer is represented as:

$$\begin{aligned}\dot{\hat{z}}_1 &= \hat{z}_2 + l_1 \sigma \epsilon_1 \\ \dot{\hat{z}}_2 &= \hat{z}_3 + l_2 \sigma \epsilon_1 \\ \dot{\hat{z}}_3 &= -a\hat{z}_1 - b\hat{z}_2 - c\hat{z}_3 + d\hat{z}_1^2 + l_3 \sigma \epsilon_1.\end{aligned}$$

In the simulation, the initial conditions  $z(0) = [1 \ -1 \ 0.1]$  and the settling time  $t_s = 2$  sec. are chosen for Figures. 3.6 and 3.7. By selecting the gains  $\alpha = 1.7$  and  $\gamma = 200$ , we assume the initial observer's states  $\hat{z}(0) = [-1 \ 5 \ 1]$  for Figure 3.6.  $\sigma = 1$

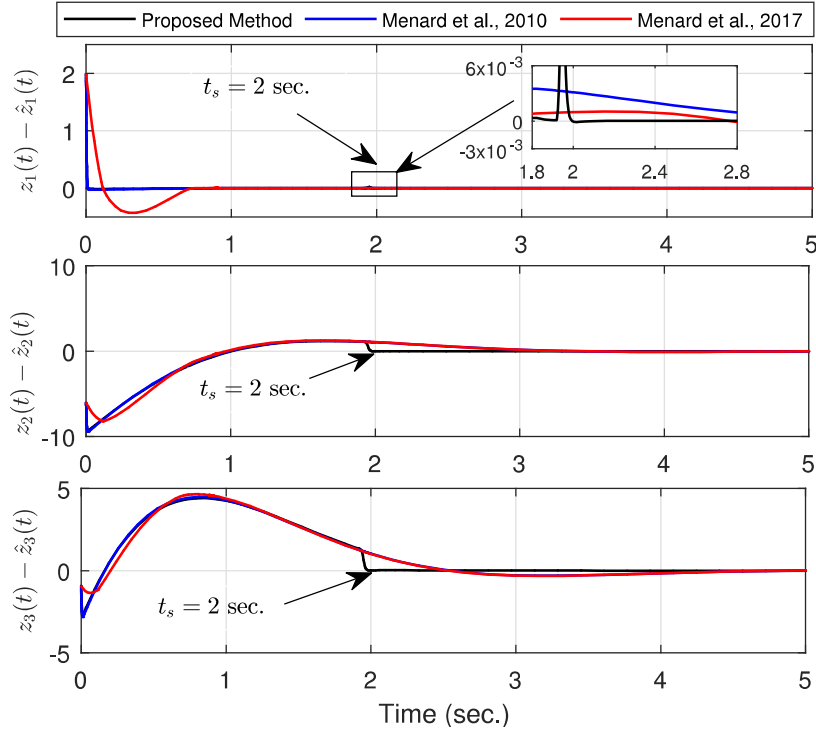


Figure 3.6: Observations error with  $t_s = 2$  sec., the initial observation states  $\hat{z}(0) = \begin{bmatrix} -1 & 5 & 1 \end{bmatrix}$ .

is selected for  $t < t_s$  and  $\sigma = 25$  is taken for  $t \geq t_s$ . The simulation results is presented in Figure 3.6. Similarly, for Figure 3.7, the gains  $\alpha = 2, \gamma = 350$  and initial conditions of the observer  $\hat{z}(0) = \begin{bmatrix} 3 & -4 & 6 \end{bmatrix}$  are selected.  $\sigma = 1$  is taken for  $t < t_s$  and  $\sigma = 220$  is chosen for  $t \geq t_s$ . The simulation results are illustrated in Figure 3.7. The time evolution of the observations error is depicted in Figures. 3.6 and 3.7. It can be clearly observed that the initial observations error for both systems are different, and the convergence time is achieved within the same desired settling time ( $t_s = 2$  sec.).

Moreover, a comparison with the global high-gain finite time observer [31] and fixed-time observer [32] has also been shown in Figs. 3.3, 3.4, 3.6, and 3.7. It is observed that the proposed method provides the convergence within the desired settling time ( $t_s = 1$  sec. in Figs. 3.3, 3.4 and  $t_s = 2$  sec. in Figs. 3.6, 3.7), which is invariant with respect to the initial conditions. Note that, the existing results on finite-time observer [31] and fixed-time observer [32] provides a larger convergence time than the proposed approach. Moreover, in finite-time observer [31], the time of convergence depends on the system's initial errors and tuning parameters whereas in fixed-time observer [32], the time

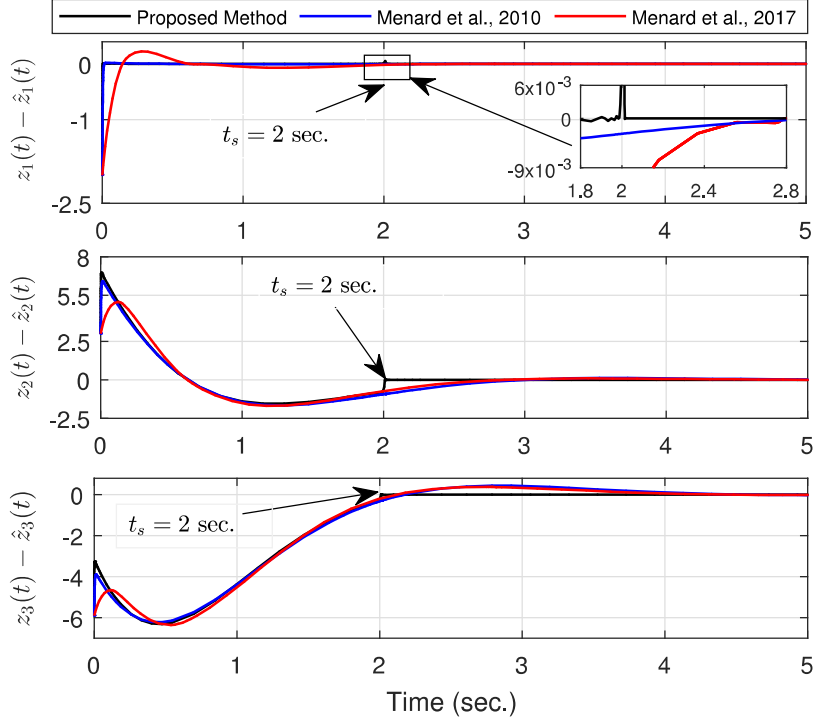


Figure 3.7: Observations error with  $t_s = 2$  sec., the initial observation states  $\hat{z}(0) = \begin{bmatrix} 3 & -4 & 6 \end{bmatrix}$ .

of convergence depends on the tuning parameters. However, in the obtained results, the convergence time is independent on the initial observations error and tuning parameters and allows the observations error to converge to zero within the chosen time  $t_s$ . This imply that the observer's state converges to the actual state within the desired time  $t_s$  without concerning the system's initial errors and tuning parameters. Moreover, the designer can choose smaller  $t_s$  for strict time-constraint problems. Therefore, it can be noticed that in the proposed approach the observation happens within the chosen time  $t_s$ . And, the designer can explicitly choose it without worrying for the initial observations error and tuning parameters.

From the above discussions, in the finite-time observer, the settling-time function depends on the initial observation error and may become large if the initial observation error is large. A solution to this problem results in a stronger notion called fixed-time observer, where the convergence time is upper-bounded with respect to the system's initial conditions. But, it is often difficult to express a direct relationship between the tuning parameters and the fixed stabilization time. Thus, the convergence time is different for

the different tuning parameters. In the proposed method, the convergence/settling time is independent with respect to the initial conditions and the time of convergence can be chosen as per our own choice. Thus, the designer can explicitly choose this desired settling time  $t_s$ . Moreover, the designer can choose smaller  $t_s$  for strict time-constraints problems.

### **3.5 Summary**

This chapter designed a switched high-gain observer with the desired convergence time for nonlinear systems. With the switching structure, the proposed observer avoids the singularity phenomena. In the obtained results, the observer's state converges to the actual state within the desired settling time  $t_s$ , and can be chosen as per our own choice. The Lyapunov theorem is used to investigate the stability analysis of the proposed approach. The simulation result of two practical systems (i) Van der Pol oscillator circuit, and (ii) Genesio-Tesi chaotic system demonstrated the effectiveness of the proposed method.